Session 1 - Cascade Testing

EXPERIMENTAL DETERMINATION OF THE INLET FLOW ANGLE OF TRANSONIC CASCADES

W. Steinert

Institut für Antriebstechnik, DLR
Linder Höhe, 5000 Köln, Germany

ABSTRACT

A method is described which enables a determination of the inlet flow angle of transonic cascades during testing. It utilizes the blade as a flow angle probe, whereby the calibration is performed by a few blade to blade calculations. The method is applicable in the subsonic and low supersonic Mach number range.

Introduction

At subsonic and supercritical inlet flow velocities flow angle probes are successfully used to determine the cascade inlet flow angle. The inlet periodicity may be checked either by traversing with a single probe or by mounting several probes in the inlet reference plane, where also the inlet velocity is measured by sidewall static taps.
Above inlet Mach numbers of about 0.8 the application of probes becomes critical and around $M_1 = 1.0$ probes would destroy the inlet flow quality completely. Unfortunately in the transonic flow range the inlet flow angle depends on the back pressure and it is therefore possible to achieve different inlet flow angles at the same geometric position of the cascade in the wind tunnel. The possible solution by measuring the inlet flow angle and velocity distributions with a Laser system is very time consuming and prohibitive for large test series. In addition it is nearly impossible to adjust the inlet flow angle in this way to a desired prescribed value. Therefore a new method for the determination of the inlet flow angle of transonic cascades had to be found.

Description of the method

Within the last years a new method has been applied successfully which relies partly on theoretical data. It is similar to the method described by Weingold and Behlke (1986) for measurements in multistage compressors and uses the theoretically predicted suction surface velocity. In fact it is utilizing the blade as a flow angle probe, whereby the calibration is performed by a flow field calculation. Therefore, the final measurement accuracy is also depending on the quality of the computer code. Another prior condition of this method is the observation that surface measurements and inviscid prediction agree quite well in the front part of the suction surface, a result which was confirmed by L2F measurements. Fig.1 shows as an example the agreement between measured and predicted surface Mach number distribution of a supercritical CDA cascade whereby the inlet flow angle was adjusted by probes and the calculation performed by an inviscid code. Differences due to viscous effects are observed generally behind 30 to 40% of chord on the suction side and along the pressure side (caused by the suction side). Therefore, a suction surface position between 5 to 20% would be best suited for these measurements. In Fig.1 the 10% position is selected with a corresponding suction surface Mach number denoted M_{ss}.

By varying the inlet flow angle (measured with reference to circumferential direction) the predicted surface Mach number distribution is changing as shown in Fig.2. All the suction surface curves are crossing nearly at one point. This is a unique feature of all subsonic and supercritical blade sections.

Therefore, at these inlet velocities the inlet Mach number may be determined also from the measured surface Mach number at this special point. Ahead of this point, the surface Mach number changes linearly with the inlet flow angle as shown in Fig.3 for the 10% chord position at different inlet flow Mach numbers. Such a favorable behaviour exists also for the gradient $d\beta_1/dM_{ss}$ of these curves which varies also linearly with M_1 up to a certain value beyond which it becomes constant (Fig.4). The latter effect is due to the well known freezing of the front surface Mach number around sonic conditions. It is clearly visible in the surface Mach number distribution of Fig.5 and even better in Fig.6 which shows the distributions of a Propfan section around sonic inlet velocities.

If the suction surface Mach number M_{ss} of the supercritical blade section is plotted as function of the inlet Mach number at a constant inlet flow angle, again a linear dependency is obtained up to the freezing condition as shown in Fig.7. By using, for instance, β_1 of Fig.7 as a constant reference value (together with the corresponding M_{ss}-curve as $M_{ss\ ref}$) as well as the dependency $d\beta_1/dM_{ss}$ of Fig.4 a simple relationship can be derived for predicting the inlet flow angle from measured suction surface and inlet flow Mach number:

$$\beta_1 = (M_{ss} - M_{ss\ ref})\, d\beta_1/dM_{ss} + \beta_{1\ ref} \qquad (1)$$

Due to the linear dependencies only four flow field calculations are required at two different inlet flow angles and corresponding inlet Mach numbers to establish the "calibration curves" of Fig.4 and Fig.7 below the freezing point around M_1 = 0.85. Beyond the freezing point $d\beta_1/dM_{ss}$ and $M_{ss\ ref}$ remain constant and two additional calculations are necessary at different inlet flow angles to cover this velocity range.

The dependency of the suction surface Mach number from the inlet flow angle at low supersonic inlet flow conditions is explained at the transonic compressor blade section L030-4 which has a design inlet Mach number of M_1 = 1.085 (Schreiber, Starken, 1984). In Figs.8 and 9 the variation of the surface Mach number distribution with inlet flow angle and inlet Mach number is shown. It can be derived from Fig.9 that between about M_1 = 0.975 and M_1 = 1.04 the velocity is constant along the front suction surface (frozen condition) and is increasing again at higher inlet Mach numbers. If the 8.9% chord position is considered with the respective surface Mach number M_{ss} the diagrams of Figs.10, 11 and 12 can be derived which describe again the relations between M_1, M_{ss}, β_1, and $d\beta_1/dM_{ss}$. It is quite evident that near linear dependencies also exist at supersonic inlet velocities. Thereby the gradient $d\beta_1/dM_{ss}$ remains constant above $M_1 > 0.97$ (Fig.12) whereas the suction surface Mach number M_{ss} increases again above a certain inlet Mach number which depends on the inlet flow angle (Fig.11). In order to establish the supersonic dependencies therefore only two additional flow field calculations are necessary at constant inlet flow angle. In Fig.11 experimentally derived data at choked condition as well as the predicted unique incidence curve are included as lower boundaries. With the aid of one curve of Fig.11 (determination of M_{ssref}) at a fixed β_1 as $\beta_{1\ ref}$ and the dependency shown in Fig.12 (determination of $d\beta_1/dM_{ss}$) an approximate but rapid prediction of the inlet flow angle is possible using again equation (1). The method is very useful because it offers the possibility to continuously calculate and observe the inlet flow angle during cascade tests by measuring only the inlet and one suction surface Mach number. The accuracy of this method depends, of course, on the accuracy of the computer code to establish the calibration curves, but also on the linear approximations and on the determination of M_1.

Verification

In order to check this method, a test series has been performed with a Propfan cascade at an inlet Mach number of $M_1 = 0.9$. Laser measurements (L2F) just upstream of the leading edge plane at three different incidences showed good agreement to the results of the above described method.
In order to proof the general validity of the method, ten different compressor cascades have been analysed theoretically at various inlet flow conditions. All cascades confirmed the near linear dependencies describéd before.

The method was applied in testing two Propfan cascades and one transonic cascade. It was possible to adjust the inlet flow angles to prescribed values. Therefore the number of test points could be substantially reduced against other test series. Furthermore this technique showed a considerable reduction of data scatter.

Conclusion

A method has been developed which permits the determination of the inlet flow angle in transonic cascades. It utilizes the blade as a flow angle probe, whereby the calibration is performed by a few blade to blade calculations. The calculations may be inviscid or viscous computations.

Acknowledgements

The author wish to thank Mrs. V. Jawtusch, Dr. R. Fuchs and Mr. A. Weber for the numerical calculations.

References

Schodl, R.: 1980: "A Laser-Two-Focus (L2F) Velocimeter for Automatic Flow Vector Measurements in the Rotating Components of Turbomachines", Trans. ASME, J. Fluid Eng., Vol. 102, No.4.

Schreiber, H.A., Starken, H., 1984, "Experimental Cascade Analysis of a Transonic Compressor Rotor Blade Section", ASME J. of Eng. for Gas Turbines and Power, Vo. 106, No. 2.

Starken, H., Jawtusch, V., 1988, "Der Machzahl- und Winkeleinfluß auf Umströmung und Verluste superkritischer Verdichtergitter", VDI-Berichte 706, VDI-Verlag Düsseldorf, pp.317 -332.

Weber, A., Steinert, W., 1989, "Experimentelle Untersuchung zweier Propfan-Gitter im transsonischen Gitterwindkanal", DLR-IB-325-08-89.

Weingold, H.D., Behlke, R.F., 1986, "The Use of Surface Static Pressure Data as a Diagnostic Tool in Multistage Compressor Development", ASME Paper 86-GT-3.

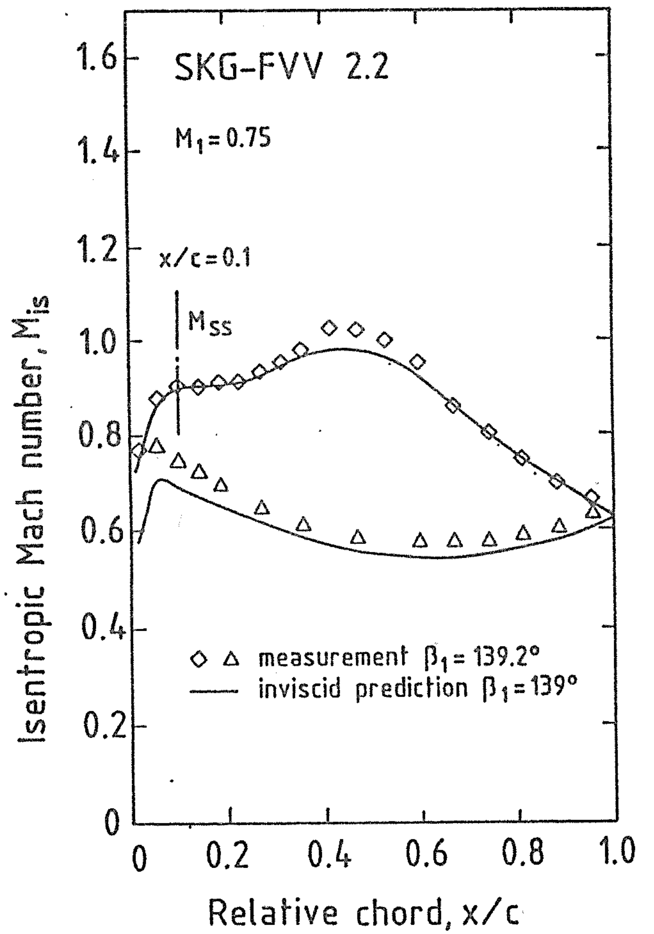

Fig.1 Measured and predicted surface Mach number distribution of a Controlled Diffusion Airfoil

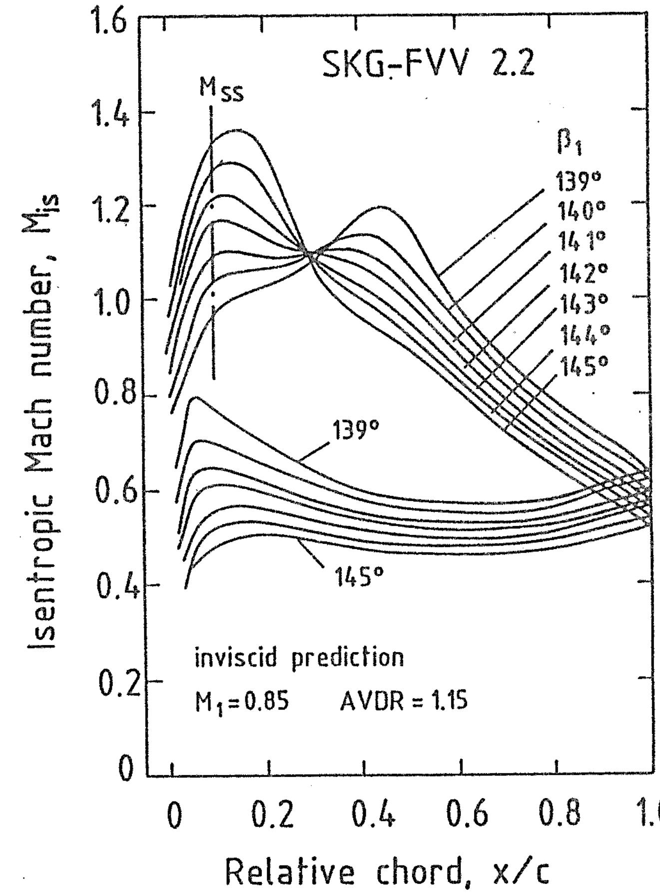

Fig.2 Surface Mach number distributions at different inlet flow angles of a Controlled Diffusion Airfoil (Starken and Jawtusch, 1988)

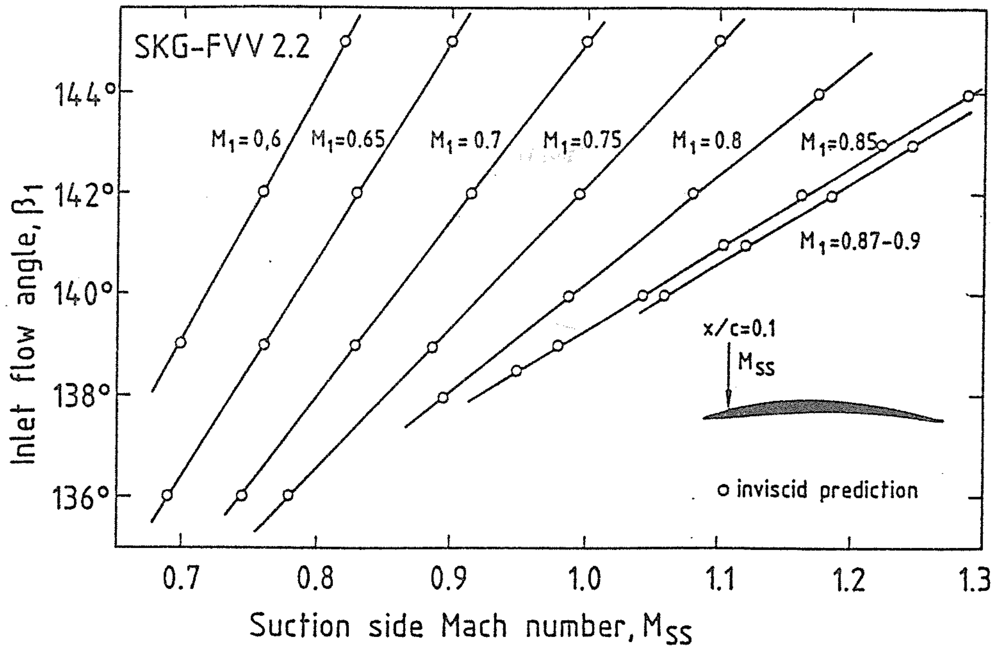

Fig.3 Inlet flow angle versus surface Mach number of a Controlled Diffusion Airfoil

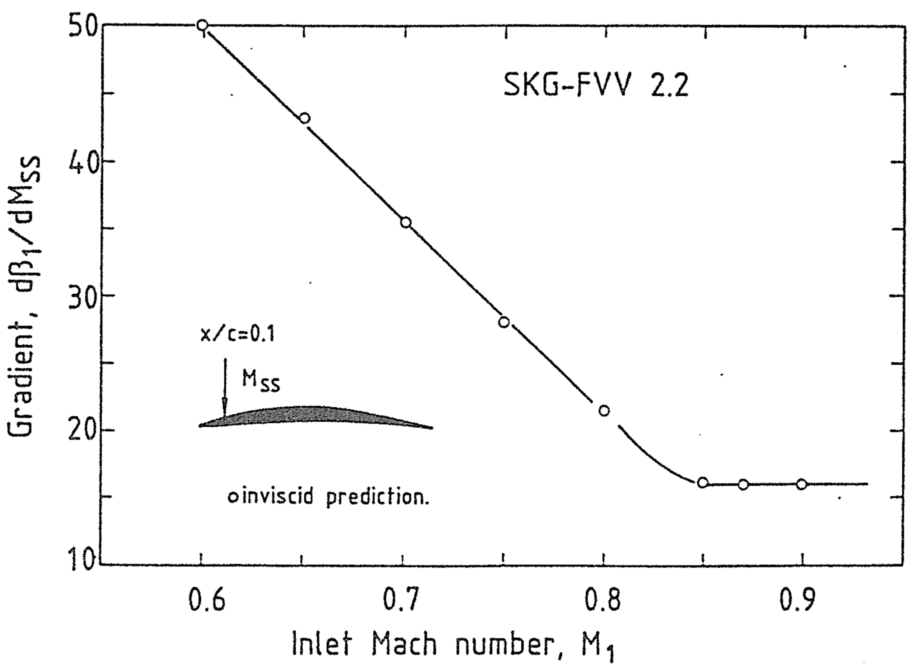

Fig.4 Gradient $d\beta_1/dM_{ss}$ versus inlet Mach number of a Controlled Diffusion Airfoil

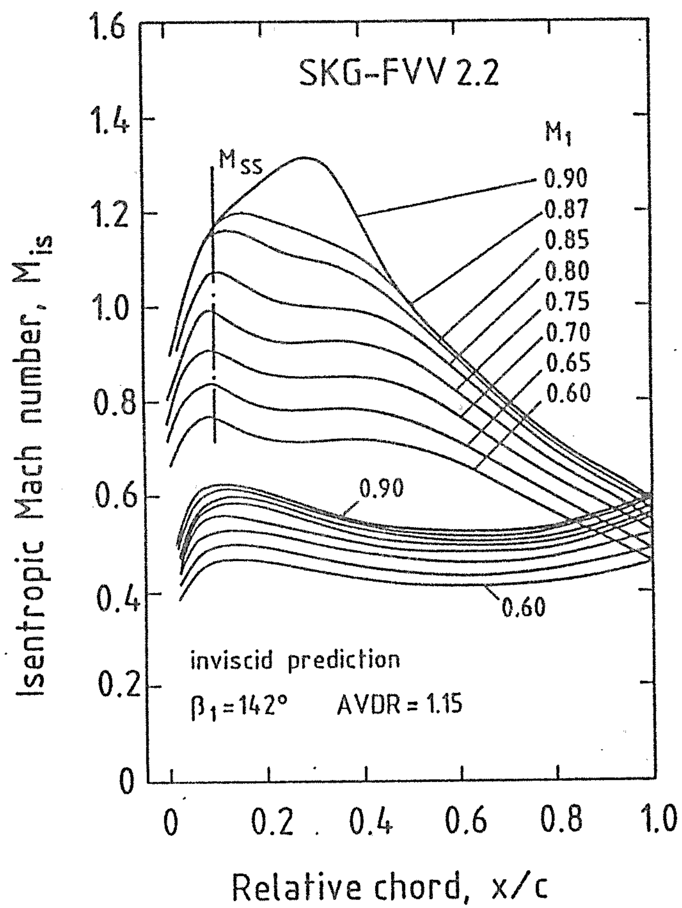

Fig.5 Surface Mach number distributions at different inlet Mach numbers of a Controlled Diffusion Airfoil (Starken and Jawtusch, 1988)

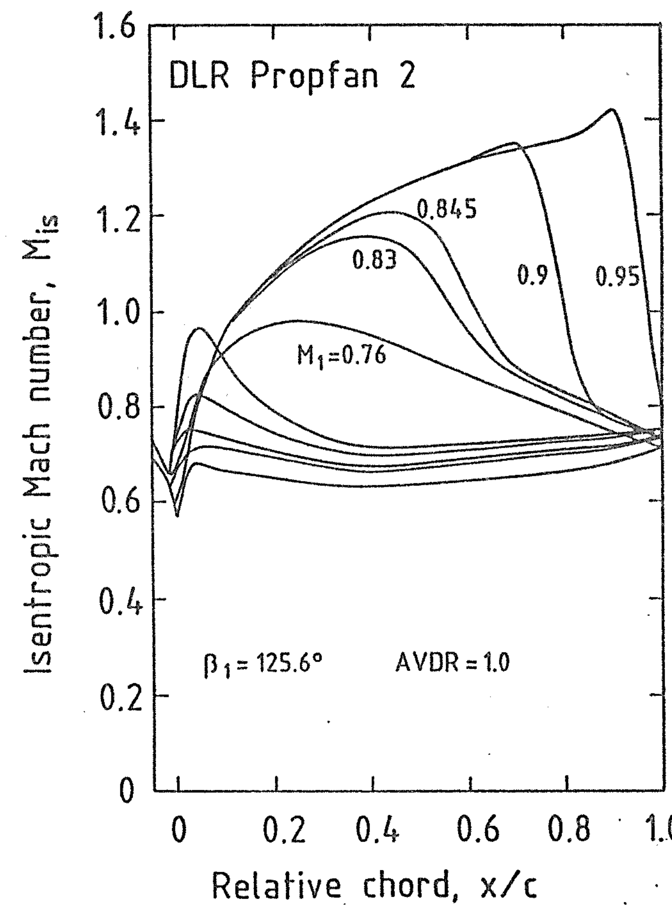

Fig.6 Surface Mach number distributions of a Propfan blade section (Weber and Steinert, 1989)

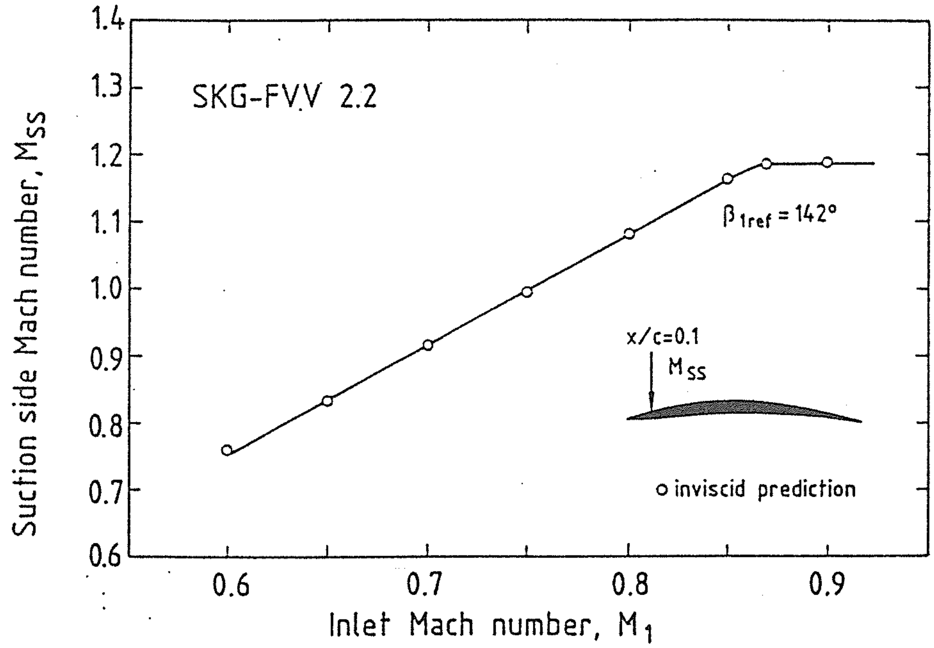

Fig.7 Suction side Mach number versus inlet Mach number of a Controlled Diffusion Airfoil

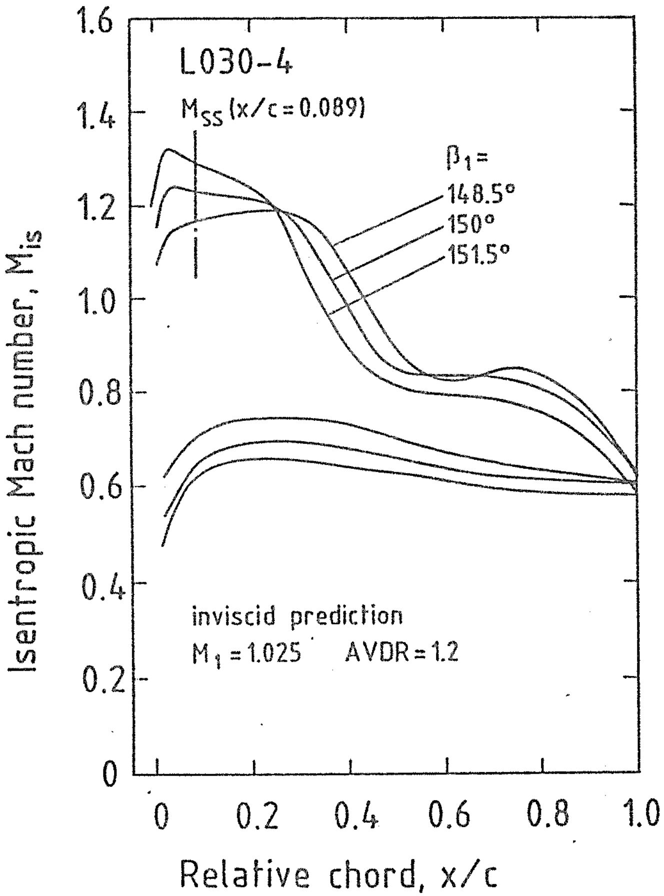

Fig.8 Variation of the surface Mach number distribution with inlet flow angle of an MCA blade section

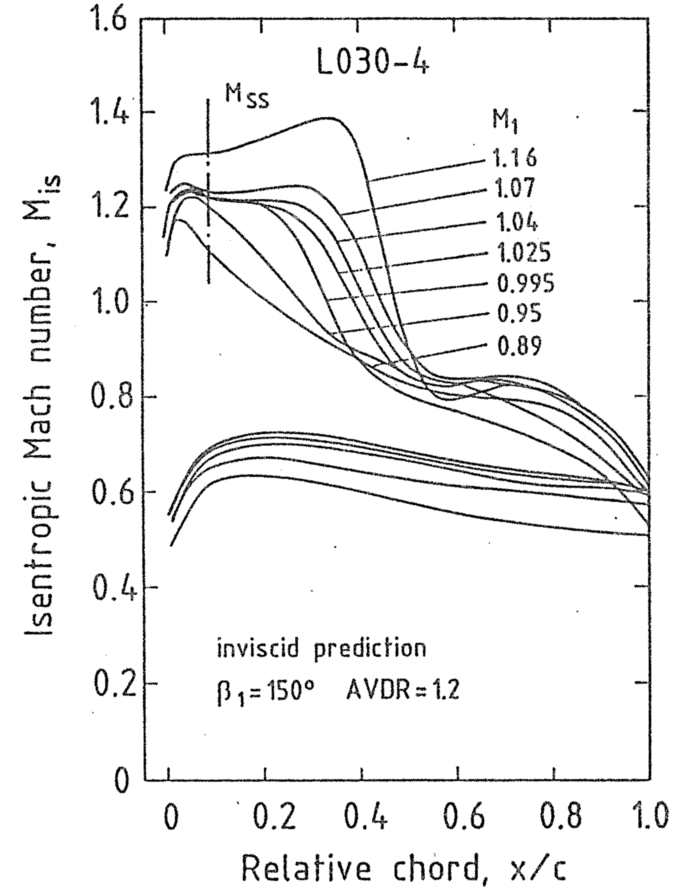

Fig.9 Variation of the surface Mach number distribution with inlet Mach number of an MCA blade section

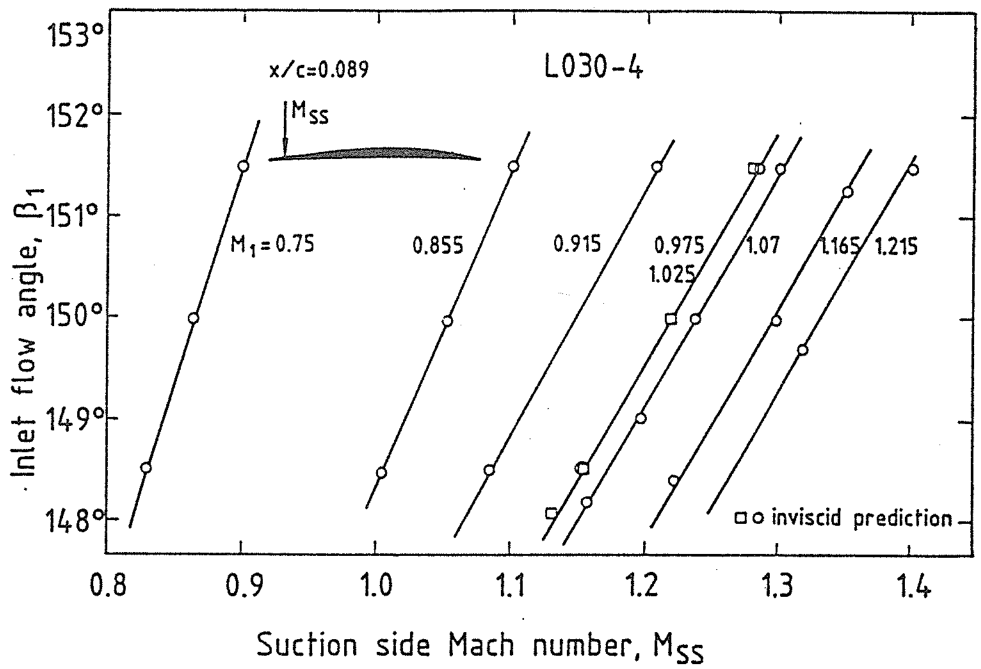

Fig.10 Inlet flow angle versus surface Mach number of an MCA blade section

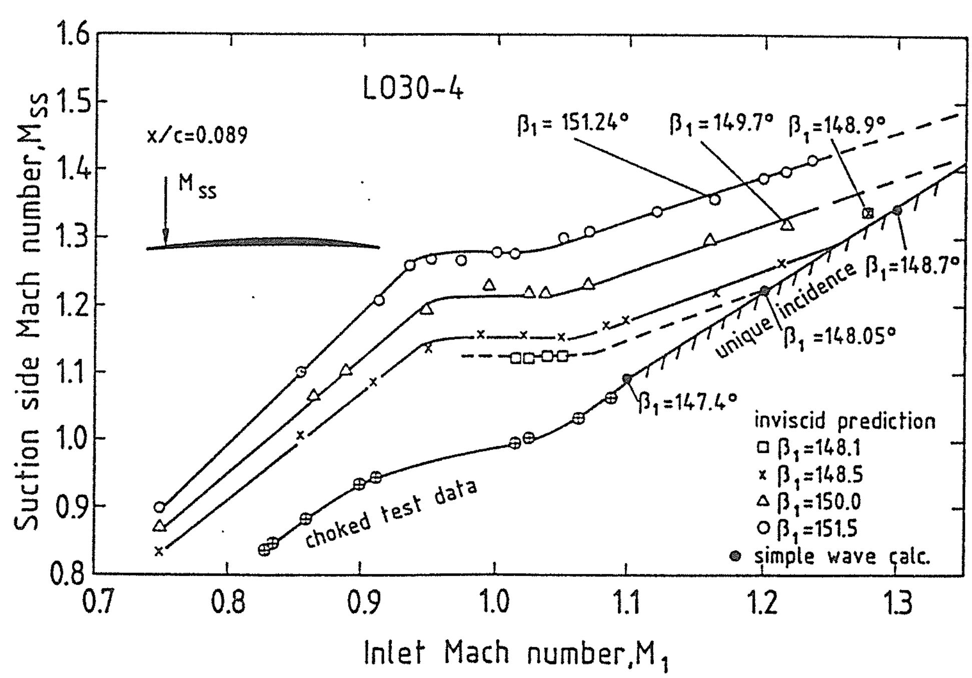

Fig.11 Suction side Mach number versus inlet Mach number of an MCA blade section

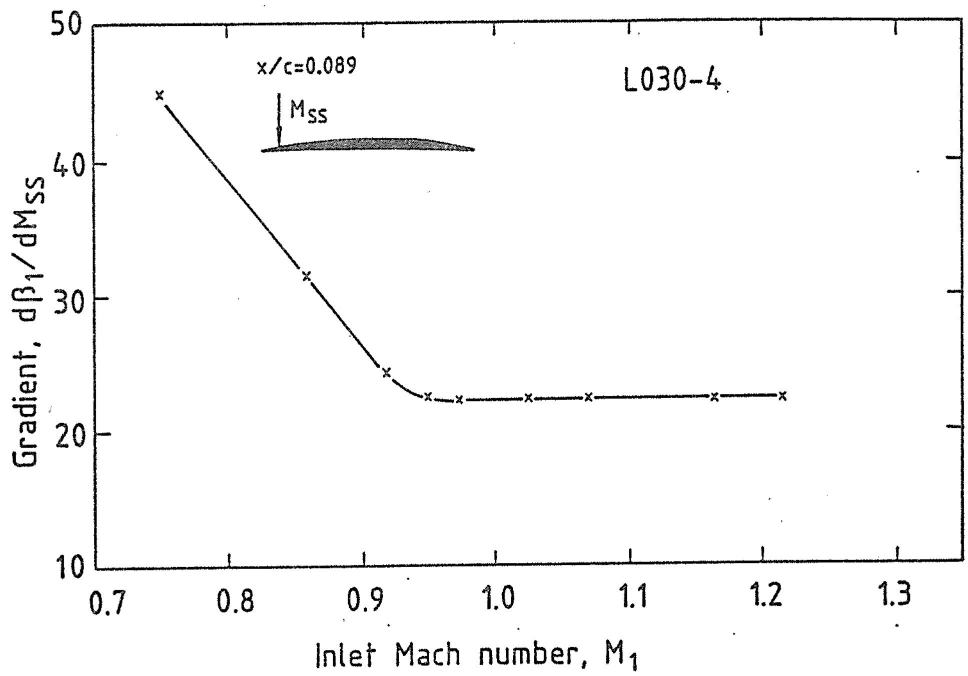

Fig.12 Gradient $d\beta_1/dM_{ss}$ versus inlet Mach number of an MCA blade section